FLAME PROPAGATION WITH HYDRODYNAMIC INSTABILITY IN VORTICAL FLOWS

K.-L. Pan

Department of Mechanical Engineering
National Taiwan University
Taipei, Taiwan 10617, R. O. C.

ABSTRACT

The interaction between a flame and vortices has been investigated by means of a front-tracking method. Extending previous studies on the role of hydrodynamic (Darrieus-Landau) instability in the wrinkling of flame surface at the incipient stage, we have further investigated the flame dynamics in the course of long-time evolution when interactions between the flame front, the instability, and the vortical flow result in highly convoluted flame configurations. It is shown that, with the inherent mechanisms of merging and dividing of flame cells at multiple scales that are generated by the hydrodynamic instability, propagation of flame wrinkles can evolve to a quasi-stable state characterized by a solitary wave or chaotic motion associated with corrugated front. If the vortical flow is sufficiently strong, however, the flame geometry is contorted by the vortices while the effect of hydrodynamic instability degenerates. Therefore, according to the relative magnitudes of the intensity of hydrodynamic instability, determined by the density ratio as well as the curvature parameter that is relevant to the flame thickness, and the strength of the vortices, the interaction pattern can be classified as flame-instability dominated, flow dominated, and a hybrid of the two.

Keywords : Flame propagation, Flame-vortex interaction, Hydrodynamic instability, Darrieus-Landau instability.

1. INTRODUCTION

In turbulent reacting flows, the deformation of flame surfaces plays a key role in the total burning rate. Its complicated behaviors, characterized by multiple scales of flame wrinkles that fluctuate both in time and space renders it difficult for quantitative analysis and prediction. In spite of this inherent complication, one may extract certain global features such as the wrinkling pattern to facilitate investigation. Conceptually, the characteristic size in turbulent flames is taken to be that of the smallest coherent structure generated by the flow, *i.e.* Kolmogorov microscale [1,2]. However, flame wrinkles may also be initiated and dominated by the hydrodynamic instability, also known as the Darrieus-Landau instability [3], on the order of the critical wavelength associated with maximum growth rate, λ_c [4], according to linear stability analysis. Indeed, this possibility was demonstrated by Cambray and Joulin [5] who numerically solved the model equation of Sivashinsky [6]. A flame passing through vortices of a continuous spectrum was simulated and the dominance of flame instability on the wrinkling scales was proposed. Nevertheless, it was found in other studies [7] on the interaction between a flame and multiple vortices that large wrinkles introduced by incident vortices prevented formation of small cells that could be excited by the hydrodynamic instability, and as such the flame was convoluted by the flow structure. This justifies the assumption of adopting turbulence scales as the wrinkling dimension in laminar flamelet regime [1,2]. These two arguments which seem contradictory to each other reveal the different mechanisms underlying the richness of flame topology in vortical flows that leads to various characteristic regimes, thus intriguing our motivation for a systematic investigation for the variation of flame pattern with respect to the critical parametric conditions. Before jumping directly into the complex flow field, however, it is desirable to know the propagation features of laminar planar flames without imposition of vortical structure, as briefly described in the following.

Linear stability analysis [8,9] shows that an initially planar flame is most unstable to perturbation with a wavelength of λ_c. Large amplitude develops subsequent to the excitation and the nonlinear dynamics dominates afterwards. Specifically, contiguous wrinkles tend to merge with each other and eventually a solitary curved flame may be created and propagate

* Assistant Professor

stably in the computational domain. If the domain size, L, is large enough, new cells are easily triggered at the crest that is associated with small curvature and weak stability. These characteristic behaviors have been demonstrated in terms of computation for the Sivashinsky equation [10-12]. Similar flame-sheet approaches that numerically solve the full field equations except those for species and energy conservations were conducted in Refs. 4 and 7. A flame thickness parameter, ℓ, was employed as a stabilizing mechanism through the flame curvature to modify the laminar flame speed, s_0, *i.e.* $s_u = s_0 (1 + \ell \nabla \cdot \mathbf{n})$. As a consequence, the curvature effect tends to filter out wrinkles of small sizes ($\lambda < \lambda_{cut}$, where $\lambda_{cut} < \lambda_c$), rendering the flame to be stable, while the flame becomes unstable for larger scales of perturbation.

If λ_c is close to the domain width, the mechanism of cell division mentioned above, known as "secondary Darrieus-Landau instability [10,13]," will not evolve and a curved flame can move stably. Nonetheless, when λ_c is much smaller than L, cells on the order of λ_c will be formed, generally around the flatter segment at the crest, and are superimposed on the large flame hump that is of the order L. Consequently the motion becomes more disordered and alternating occurrence of merging and splitting of wrinkles appear. Thus the transition criteria would be related to L and λ_c as well as the intensity of hydrodynamic instability as represented by the density ratio q and ℓ. Here we have excluded the effect of absolute flame speed which is normalized to unity in the computation. Meanwhile, the potential influence of thermal-diffusive instability due to unequal rates of heat and mass diffusion is not considered herein, which is not uncommon to myriads of mixtures in stoichiometric conditions.

To further study the interaction between flames and vortices, we have adopted a front-tracking numerical method [14,15] that is based on the flame-sheet approach while allows for reasonably large density jump across the flame and associated nonlinear dynamics. Owing to simplification of the governing equations, direct implementation of flame propagation mechanism, and well-controlled vortical flow structure, the underlying physics can be readily extracted, thereby providing a first insight into the complicated evolution of turbulent flame topology. Furthermore, the study serves as a continuation of our previous work [4] on the incipient evolution of flame-vortex interaction, so as to track the ensuing long-time behaviors particularly the characteristic patterns of flame wrinkling in vortical flows. Through the investigation of the velocity and pressure fields, additional insight is gained into the nonlinear structure such as merging of contiguous cells.

2. FORMULATION

The numerical approach is based on the front-tracking method developed for multiphase flows [16] and modified [14,15] to simulate the propagation of a premixed flame surface in arbitrary flow field, allowing for thermal expansion across the flame and its subsequent influence on the hydrodynamics. The conservation equations of mass and momentum are written for the entire domain in two-dimensional coordinates (x, y) as:

$$\nabla \cdot \rho \mathbf{u} = \int_f \Delta\rho (s_u \mathbf{n} - \mathbf{u}_f) \cdot \mathbf{n} \delta(\mathbf{x} - \mathbf{x}_f)\, dl \qquad (1)$$

$$\frac{\partial \rho \mathbf{u}}{\partial t} + \nabla \cdot \rho \mathbf{u}\mathbf{u} = -\nabla p + \nabla \cdot \left[\frac{1}{Re} (\nabla \mathbf{u} + \nabla^T \mathbf{u}) \right] \qquad (2)$$

where ρ and p are the dimensionless density and pressure, with $\Delta\rho$ being the difference between the densities of the unburned and burned mixtures, and Re the Reynolds number. The flow velocity, u, is normalized by the laminar flame speed of methane at atmospheric condition, *i.e.* $s_0 = 8$ cm/s. The integration in Eq. (1) is over the whole flame surface and includes thermal expansion on the velocity divergence, where $\delta(\mathbf{x})$ is a two-dimensional delta function defined on the position vector $\mathbf{x}$, with $\mathbf{x}_f$ being the flame surface and $\mathbf{n}$ the unit normal vector of the flame front directing toward the burned side. Thus by integrating Eq. (1) over the flame surface a source term is obtained which yields the jump of the normal velocity across the flame. The singular source of the divergence of the mass flux is smoothed across the flame in terms of the immersed-boundary method [17] but is rendered zero away from the surface. The interface is represented by separate computational points that move with the flame speed relative to the local flow velocity interpolated from the grid. These points are connected to form a front which keeps the density and viscosity stratifications sharp.

A normalized speed of curvature-affected flame propagation is used, given by $s_u/s_0 = 1 + \ell \nabla \cdot \mathbf{n}$ [8], where ℓ characterizes the ratio of flame thickness to the hydrodynamic scale, Λ, which is taken to be 1cm. By assigning a weak curvature effect, with $\ell \ll 1$, the formation of sharp corners over the flame surface is prevented while a stabilizing mechanism for the hydrodynamic instability is provided. It is noted that the flame speed is in fact a function of the stretch in the first-order approximation [8,9]. In the current study with negligible difference in the transfer rates of heat and species, however, the stretch can be merely represented by the curvature term and thus the coefficient ℓ corresponds to the well known Markstein length [18].

The interaction between the flame and the vortical flow was studied with Oseen vortices superimposed in the velocity field. They were imposed either as initial conditions or as the inlet boundary condition (at $y = 0$) to simulate a stream of continuous vortices. For a single Oseen vortex, the vorticity strength, ω, and the azimuthal velocity, v_θ, are respectively given by

$$\omega = \frac{\Gamma_0}{\pi} \exp(-r^2/R^2), \quad v_\theta = \frac{\Gamma_0}{2\pi r} \left[1 - \exp(-r^2/R^2) \right], \qquad (3)$$

where Γ_0 is the initial total circulation, R the characteristic vortex radius, and r the radial distance from the vortex core center. The normalized velocity v_θ, which is the ratio of the rotational flow velocity to the laminar flame speed, vanishes at the vortex center, $r = 0$, and far away, $r \to \infty$, and achieves a maximum value $v_{\theta,m} = 0.1016$ (Γ_0 / R) at $r_m \cong 1.1209R$. It is noted that the inlet velocity of flow was implemented according to the average speed of flame propagation, s_a, which was calculated in terms of the total burning rate divided by the domain width, L. Therefore the flame can be anchored at the central region of the computational domain and the long-term evolution can be tracked.

3. RESULTS AND DISCUSSION

3.1 Flame Passage through a Pair of Vortices

We start to see the evolution of a flame surface after passing a pair of vortices. We are particularly interested in the role of initial perturbation in the excitation of flame wrinkling via the hydrodynamic instability, leading to more rapid attainment of the nonlinear stage that shows characteristic pattern of interest.

3.1.1 Quasi-Stable State

Figure 1 is the superposition of flame fronts that are separated by a specified distance for visual clarity. It is seen that, when a flame passes a vortex pair, it is first wrinkled at the center, amplified by the hydrodynamic instability [4]. Furthermore, two curved corners are created at the shoulders, and then develop and propagate toward the periodic boundaries. They are merged, forming a wrinkle stabilized at the boundary. This condition is referred to a "metastable state," in the recognition that, after some time being at this state, the central wrinkle moves toward one of the boundaries and the symmetry is broken, as shown in the right panel for $t > 40$. The wrinkles eventually merge and thereafter only a single curved flame appears, propagating stably in the domain. This is an inert pattern with almost invariant flame geometry, analogous to curved flames propagating in tubes [19-21]. We shall designate this regime as that of "quasi-stable state".

The shape and magnitude of the front in the quasi-stable state are independent of the vortex structure such as size, strength, and configuration, while they are determined by the evolution of hydrodynamic instability that is related to gas expansion via the density variation across the flame, curvature effect, and the domain size. We first assume that three length scales characterize the evolution, *i.e.* λ_c, L, and the perturbation wavelength imposed by the vortex structure ($\lambda_p \approx 4\ r_m$). It was found that the influence of λ_p was only important at the early stage when the flame was deformed by the vortical flow. If λ_p is close to λ_c, the wrinkle is readily amplified by the hydrodynamic instability [4]. Then the disturbances are dispersed outward to the boundaries as a consequence of local flow motion, as will be further demonstrated in later sections. Eventually troughs saturated in the shape (curvature) due to the balance between the flow and flame motion are formed at the center and the boundary, associated with wavelengths of the order λ_c. As shown in Fig. 1, this state may last for a long time, depending on the relative separation, characterized by two wrinkles with metastability. The stability is dominated by the ratio between L and λ_c, and the effect of hydrodynamic instability that would be presumably grouped into a single dimensionless parameter, $I(q, \ell)$, which is somehow related to its growth rate. Generally if λ_c / L is not too large or significant perturbation is introduced, as shown in Fig. 2 for an incident vortex pair with maximum swirling velocity $v_{\theta,m} = 1/8$, the metastability is destroyed quickly and the second stage is triggered, at which the two wrinkles move toward each other and coalesce, leading to a quasi-stable state. A stable flame trough is then formed and propagates steadily as long as λ_c / L is sufficiently large. Further complication can be rendered by $I(q, \ell)$, which is however not able to be determined exactly based on the present simulation results, though it may have similar effect as λ_c / L, and a challenging nonlinear analysis would be needed to extract a grouped dimensionless parameter if it ever exists. It is noted that λ_p plays no role in the final flame geometry. Thus while the vortices provide incipient perturbation for the flame wrinkling, their influence is eventually lost after some time.

3.1.2 Chaotic State

If λ_c / L is sufficiently small, *e.g.* due to a small ℓ, new cells caused by secondary Darrieus-Landau instability shall be generated at the crest after the wrinkles are merged, as shown at the intermediate instants in the right column of Fig. 3. The new cell subsequently moves toward a nearby wrinkle and merges again. The merging and dividing of cells become more frequent as λ_c / L is further reduced. Figure 4 indicates that small cells are intermittently created and superimposed on the large background hump. The large wrinkles, inducing stronger non-uniform flow motions, continuously attract

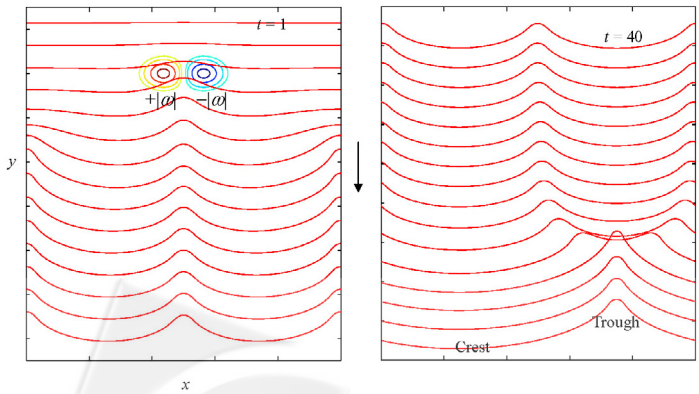

Fig. 1 Evolution of an initially planar flame passing through a vortex pair ($\ell = 0.15$, $q = 5$), with initial vorticity contours plotted as well. The time difference (Δt) is 1 but is increased to 2 after $t > 40$

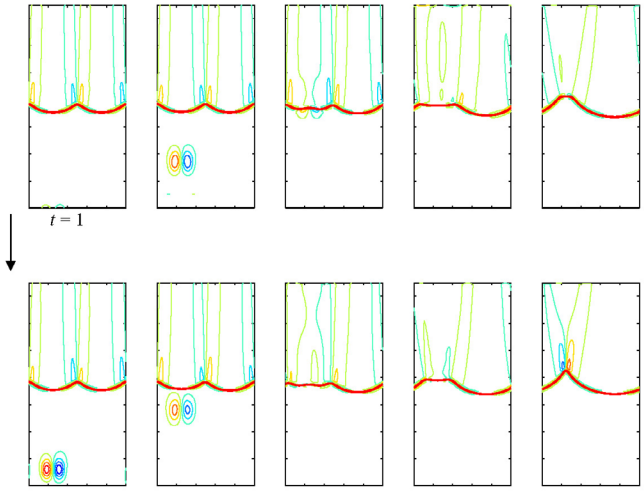

Fig. 2 The evolution of flame shape with vorticity contours for a curved flame impacted by a vortex pair ($\ell = 0.1$, $q = 2$, $v_{0,m} = 1/8$, $\Delta t = 2$)

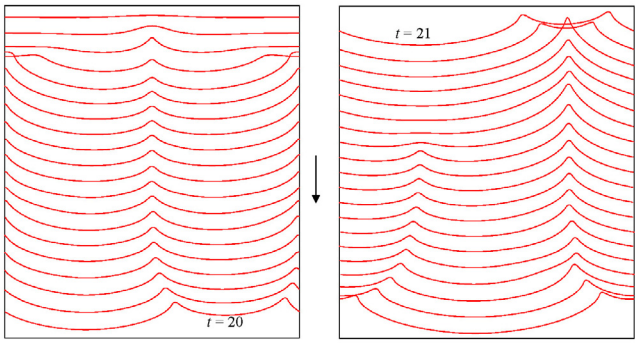

Fig. 3 Evolution of an initially planar flame passing a vortex pair ($\ell = 0.05$, $q = 5$, $\Delta t = 1$)

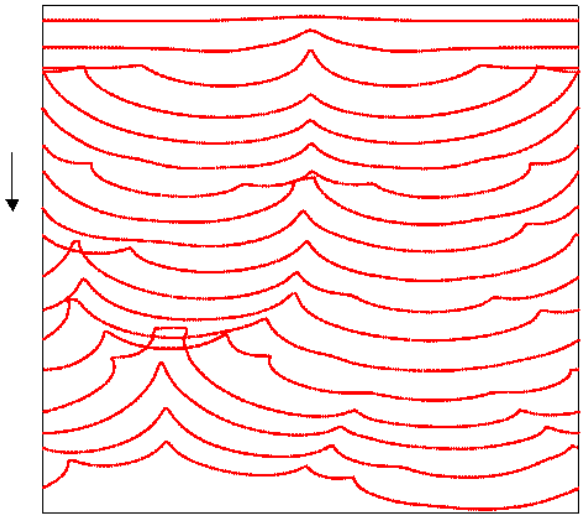

Fig. 4 Evolution of an initially planar flame passing a vortex pair ($\ell = 0.01$, $q = 5$, $\Delta t = 1$)

and engulf small cells. The unsteady motion becomes more prominent if the size of the background hump is comparable to those of the instability-induced cells since their interactions are manifested somehow.

Similar to the quasi-stable state, no effect is left from the initial vortex structure on the subsequent evolution of the flame pattern, which is controlled by the hydrodynamic instability as that without perturbation of vortices.

3.2 Mechanistic Interpretation of Merging and Dividing of Flame Wrinkles

It is seen that the long-time behavior of flame evolution may be characterized by persistent merging and dividing of wrinkles. New cells tend to be generated in smooth regions such as the broad crests. This is analogous to the excitation of λ_c cells in the propagation of a planar flame. Since the local curvature is small, the stretch exerted on the flame surface is not strong enough to suppress the evolution of hydrodynamic instability as that in [7,22]. Furthermore, perturbations tend to be created by the kinks associated with high-order variations (derivatives) of flow properties such as the velocity and pressure, which connect the smooth crests associated with small curvature and the curved segments where the incoming flow is turned toward the troughs. This is somehow analogous to the onset of a Tollmien-Schliting wave, which is an indication of laminar-flow instability and a precursor of transition to turbulence [23]. Around the high-order inflexion points, perturbations are readily produced, providing sources to trigger the hydrodynamic instability and the subsequent evolution of flame wrinkles. These wrinkles then travel along the flame surface due to asymmetric balance of the local flow field that will be described in next paragraph. This form of perturbation waves can be somehow demonstrated by analyzing the Sivashinsky equation [6], which justifies the existence of slow traveling wave solutions that lead to chaotic evolutions observed numerically [24].

In crowded zones, contiguous cells tend to merge. Mathematically, this can be interpreted by the pole dynamics in terms of pole decomposition [25,26], in that the poles on the imaginary axis in the complex domain are attracted by the steady ones toward the real axis. Mechanistically, it is triggered by disturbances that result in asymmetric imbalance, which introduces traversing motion and encourages merging of neighboring wrinkles. This can be demonstrated by the velocity field as shown in Fig. 5, which corresponds to $t = 22$ as shown in Fig. 3. It is seen that if the symmetry of the flame is slightly broken, the incoming flow structure becomes asymmetric. It imparts a transverse component to the flow velocity moving toward the trough of the flame, and thus further inclines the wrinkle, as indicated in Fig. 5 by the left segment of the flame with incoming flow toward the right side. As a consequence, more fluid is attracted from the crest toward the trough and the slant is further enhanced. The amplification on the asymmetry caused by initial perturbation

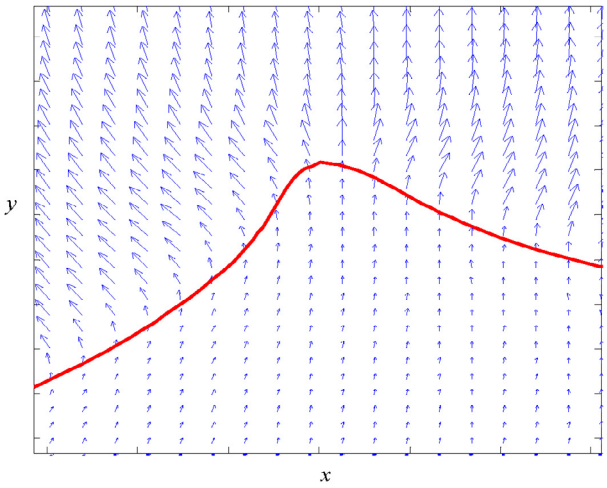

Fig. 5 Flame geometry and velocity vectors during the merging of contiguous wrinkles ($\ell = 0.05$, $q = 5$, $t = 22$)

thus results in substantial inclination of the flame surface and nontrivial net velocity in the x direction, leading to traversing movement of the flame and eventually merging of contiguous wrinkles, of either comparable or distinct amplitudes as well as length scales. The latter case for disparate scales has been shown by Zel'dovich *et al*. [19] and Helenbrook and Law [7], who explained the motions of small cells engulfed by large wrinkles in terms of the sweeping of the flow within the large wrinkles. It is included in our interpretation, in that the asymmetric disturbance is now a consequence of the flowing with predominant direction generated by the large wrinkle. To study this mechanism unambiguously, a controlled perturbation in the form of a weak stream toward the crest was introduced. As shown in Fig. 6(a), the left crest on the flame is lifted, by which the flame segments in the left domain are slanted and indeed move laterally toward each other. Furthermore, if the clockwise rotating vortex at the right of the original pair is 1% stronger, as shown in Fig. 6(b), the incoming flow toward the central trough is not symmetric and the wrinkle is tilted. It subsequently slides to the right boundary by the non-uniform flow velocity and merges with the other wrinkle moving in the opposite direction. The movement of the wrinkles can also be interpreted by the pressure difference between the unburned fluids within the two troughs.

3.3 Flame Passage through Continuous Vortices

To further study the interaction between a flame and vortices, a stream of vortex pairs was introduced from the inlet boundary. Figure 7 shows that if the vortices are weak, the flame front, which is originally at the metastable state, is slightly wrinkled by the incident vortices. While the hydrodynamic instability introduces further excitation and evolution for the wrinkles, the surface is weakly distorted since the growth rate of the instability as well as its intensity are small. When ℓ is

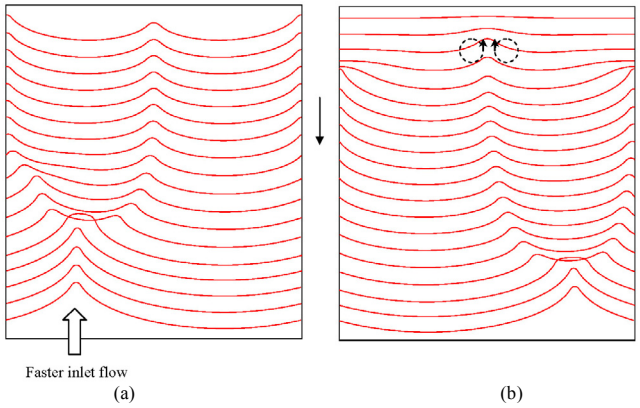

Fig. 6 Evolution of a flame initially perturbed by a vortex pair ($\ell = 0.1$, $q = 5$, $\Delta t = 1$): (a) perturbed later by asymmetric inlet flow with velocity 10% faster at the center of the left entrance section; (b) the incipient vortex pair is not symmetric, in which the right vortex is 1% stronger

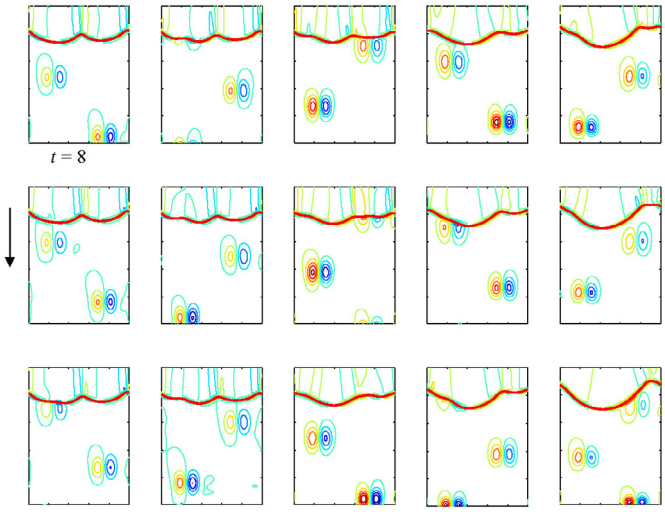

Fig. 7 The evolution of flame shape with vorticity contours for a curved flame impacted by continuous vortex pairs ($\ell = 0.1$, $q = 2$, $v_{\theta,\,m} = 1/8$, $\Delta t = 1.0$)

decreased, indicating a thinner flame and hence weaker stabilization via curvature, the flame becomes more unstable and sharper wrinkles are formed. As shown in Fig. 8, while the flame is weakly perturbed by the vortices, the wrinkles quickly develop to cells associated with saturated magnitude and curvature, which are attracted by the large troughs in terms of the mechanisms discussed. As a consequence, the formation of wrinkles induced by the hydrodynamic instability is related to the striking frequency of the vortices. Meanwhile, it is expected to depend on the relaxation time of the strained vortical flow as well as the growing rate of the incipient wrinkles toward developed cells. If the period between the incident vortices is short, the hydrodynamic instability will not have sufficient time to

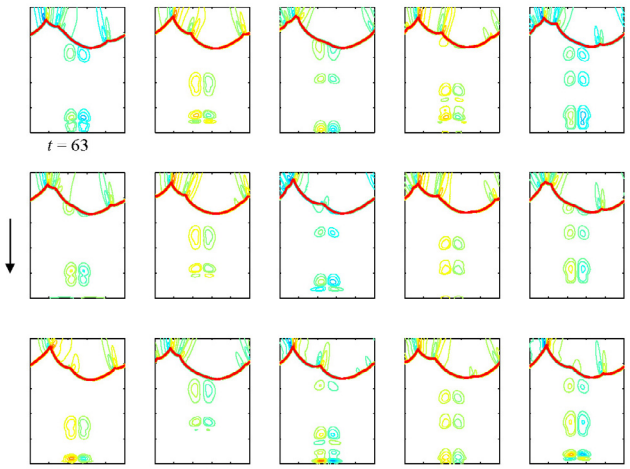

Fig. 8 The evolution of flame shape with vorticity contours for a curved flame impacted by continuous vortex pairs ($\ell = 0.01$, $q = 2$, $v_{0,m} = 1/8$, $\Delta t = 0.8$)

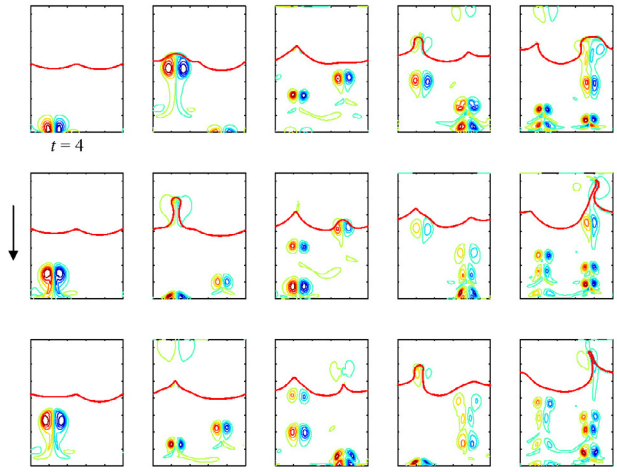

Fig. 9 The evolution of flame shape with vorticity contours for a curved flame impacted by continuous vortex pairs ($\ell = 0.1$, $q = 2$, $v_{0,m} = 2$, $\Delta t = 1.0$)

develop cells. Therefore the flame geometry is convoluted to the vortical flow structure, as assumed for the laminar flamelet regime in the modeling of turbulent flames [1,2].

It is further noted that, while the length scale initially perturbed by the vortices is moderately larger than λ_c ($\lambda_p/\lambda_c \approx 5$ for $q = 2$ and $\lambda_p/\lambda_c \approx 10$ for $q = 5$ as we have tested), wrinkles of the order λ_c can still be developed by the hydrodynamic instability. However, if the difference is too large, the time for the perturbations to evolve to cells becomes relatively long, which may not then materialize in the presence of the external flow. Specifically, when the vortical flow is sufficiently strong, the straining effect will inhibit the development of λ_c cells via the hydrodynamic instability, in accordance to the arguments of Helenbrook and Law [7] that small cells cannot be excited by vortices of much larger sizes ($\lambda_p/\lambda_c = 10$ for $q = 2$).

3.4 Flame Interaction with Strong Vortices

It is seen that if the strength of the incident vortices is small, cells of the order λ_c are induced by the hydrodynamic instability. It is also shown that small cells can be generated by perturbations of vortices up to moderately large scale while their sources are somehow different from those inherently formed on planar flames due to noises. Specifically, perturbation waves are excited by the disturbances of vortices even with scales larger than λ_c, which gradually evolve to saturated wrinkles of the order λ_c during their movement toward the large troughs; thus the frequency is contingent upon the impact of vortices. As the vortex strength is sufficiently large, however, the flame surface is convoluted to that of the driving flow, as shown in Fig. 9. The external flow dominates the motion of the flame front and even leads to formation of unburned pockets [27], as demonstrated by the breaking of the substantially distorted neck (*e.g.* between $t = 8$ and 9 in which the remnant of vorticity is left from the burn-down of the pocket). While the hydrodynamic instability may not introduce flow locally that is strong enough to compete with the external flow, it can somewhat enhance the growth of flame wrinkles [7].

4. CONCLUDING REMARKS

We have studied numerically the characteristic patterns when a flame front propagates in vortical flows as an elemental process representing the interaction between flames and turbulent flows. While the flame maintains a locally laminar structure, its burning speed is modified through the curvature. Thus the long-time evolution can be studied via the nonlinear mechanisms of the stabilization of curvature and destabilization of the hydrodynamic instability. It is shown that, depending on the intensity of the hydrodynamic instability, the domain size, and the strength of vortices, the global characteristics can be classified as those dominated by the hydrodynamic instability, the vortical flow, or by both. When the external flow is relatively weak or moderate, the geometrical evolution of the flame is dominated by the hydrodynamic instability. Depending on the ratio between λ_c and L as well as possible complication of the intensity of hydrodynamic instability that is related to q and ℓ, the flame shall propagate either steadily or unsteadily in the computational domain, with the latter being characterized by incessant merging and dividing of wrinkles. If the vortex is sufficiently strong, however, the hydrodynamic instability does not have enough time to effect wrinkling of the flame surface, which ultimately conforms to the contortion of the vortical flow motion. It justifies the adoption of the smallest coherent structure as the wrinkling scale of turbulent flame in the laminar flamelet regime.

We have further investigated the flow structure of merging and splitting of flame wrinkles as the long-time outcome of the nonlinear evolution. It was found that asymmetrical perturbations to the metastable wrinkles can trigger transverse traveling through the imbalance between the local flow and flame motion, and hence contiguous cells tend to merge. Furthermore, in smooth regions where the curvature is small, the flame surface is sensitive to perturbations that generate kinks and provide sources for traveling waves on the surface, which then develop to cells of the order λ_c due to the hydrodynamic instability. Consequently, as supplement to previous arguments [7], new wrinkles can still be formed around the crests associated with small curvature by moderately large vortices, and as such are not only vulnerable to the most "dangerous" wavelength of perturbation, *i.e.* λ_c. In a sense, the occurrence of new cells are related to the striking of incident vortices while their shape and scale are determined by the hydrodynamic instability, since the flame configuration is balanced by the flame motion modified by the curvature and the local flow as a function of the density ratio, which characterizes the instability structure.

ACKNOWLEDGEMENTS

The author thanks Professor C. K. Law for helpful discussion on this work.

NOMENCLATURE

ℓ	curvature coefficient
L	width of the computational domain
n	unit normal vector directing toward the burned gas
p	pressure
q	density ratio of unburned to burned gases
r	radial distance from the vortex core center
r_m	radial distance from the vortex core center when v_θ is maximum
R	characteristic radius of an Oseen vortex
Re	Reynolds number
s_0	laminar flame speed
s_a	average flame speed
s_u	flame speed relative to the unburned gas
t	time
u	flow velocity vector
u_f	flow velocity at the flame front
v_θ	azimuthal vortex velocity
$v_{\theta,\,m}$	maximum swirling velocity
x	position vector

Greek Symbol

α	growth rate of perturbation on flame front
$\delta(\mathbf{x})$	two-dimensional delta function defined on the position vector **x**
ρ	density
ω	vorticity strength
λ_c	the critical wavelength associated with maximum growth rate
λ_{cut}	the cutoff wavelength associated with zero growth rate
λ_p	wavelength of perturbation rendered by the incident vortices
Λ	characteristic length scale used for normalization
Γ_0	initial total circulation

REFERENCES

1. Peters, N., "Laminar Flamelet Concepts in Turbulent Combustion," *Proc. Combust. Inst.,* 21, pp. 1231−1250 (1986).
2. Gouldin, F. C., "An Application of Fractals to Modeling Premixed Turbulent Flames," *Combust. Flame*, 68, pp. 249–266 (1987).
3. Landau, L. D. and Lifshitz, E. M., *Fluid Mechanics,* 2nd Edition, Oxford, Butterworth-Heinemann, Chap. 14 (1987).
4. Pan, K. L., Qian, J., Law, C. K. and Shyy, W., "The Role of Hydrodynamic Instability in Flame-Vortex Interaction," *Proc. Combust. Inst.*, 29, pp. 1695−1704 (2002).
5. Cambray, P. and Joulin, G., "Length-Scale of Wrinkling of Weakly-Forced, Unstable Premixed Flames," *Combust. Sci. Tech.,* 97, pp. 405−428 (1994).
6. Sivashinsky, G. I., "Nonlinear Analysis of Hydrodynamic Instability in Laminar Flames — I. Derivation of Basic Equations," *Acta Astronautica*, 4, pp. 1177−1206 (1977).
7. Helenbrook, B. T. and Law, C. K., "The Role of Landau-Darrieus Instability in Large Scale Flows," *Combust. Flame*, 117, pp. 155−169 (1999).
8. Law, C. K. and Sung, C. J., "Structure, Aerodynamics, and Geometry of Premixed Flamelets," *Prog. Energy Combust. Sci.,* 26, pp. 459−505 (2000).
9. Pelce, P. and Clavin, P., "Influence of Hydrodynamics and Diffusion Upon the Stability Limits of Laminar Premixed Flames," *J. Fluid Mech.*, 124, pp. 219−237 (1982).
10. Denet, B., "On Non-Linear Instabilities of Cellular Premixed Flames," *Combust. Sci. Tech.,* 92, pp. 123−144 (1993).
11. Gutman, S. and Sivashinsky, G. I., "The Cellular Nature of Hydrodynamic Flame Instability," *Physica D,* 43, pp.

129−139 (1990).
12. Michelson, D. M. and Sivashinsky, G. I., "Nonlinear Analysis of Hydrodynamic Instability in Laminar Flames — II. Numerical Experiments," *Acta Astronautica,* 4, pp. 1207−1221 (1977).
13. Bychkov, V. V. and Liberman, M. A., "Dynamics and Stability of Premixed Flames," *Phys. Rep.*, 325, pp. 115−237 (2000).
14. Qian, J., Tryggavason, G. and Law, C. K., "A Front Tracking Method for the Motion of Premixed Flames," *J. Comput. Phys.*, 144, pp. 52−69 (1998).
15. Pan, K. L., Shyy, W. and Law, C. K., "An Immersed-Boundary Method for the Dynamics of Premixed Flames," *Int. J. Heat Mass Transfer,* 45, pp. 3503−3516 (2002).
16. Unverdi, S. O. and Tryggvason, G. A., "Front-Tracking Method for Viscous, Incompressible, Multi-Fluid Flows," *J. Comput. Phys.*, 100, pp. 25−37 (1992).
17. Peskin, C. S., "Numerical Analysis of Blood Flow in the Heart," *J. Comput. Phys.*, 25, pp. 220−252 (1977).
18. Markstein, G. H., *Non-Steady Flame Propagation,* Pergamon, p. 22, New York (1964).
19. Zel'dovich, Y. A. B., Istratov, A. G., Kidin, N. I. and Librovich, V. B., "Flame Propagation in Tubes: Hydrodynamics and Stability," *Combust. Sci. Tech.,* 24, pp. 1−13 (1980).
20. Denet, B., "Intrinsic Instabilities of Curved Premixed Flames," *Europhys. Lett.,* 21, pp. 299−304 (1993).
21. Bychkov, V. V., Golberg, S. M., Liberman, M. A. and Eriksson, L. E., "Propagation of Curved Stationary Flames in Tubes," *Phys. Rev. E,* 54, pp. 3713−3724 (1996).
22. Sivashinsky, G. I., Law, C. K. and Joulin, G., "On Stability of Premixed Flames in Stagnation-Point Flow," *Combust. Sci. Tech.*, 28, pp. 155−159 (1982).
23. White, F. M., *Viscous Fluid Flow*, 2nd Edition, Singapore, McGraw-Hill Inc., Chap. 5 (1991).
24. Novick-Cohen, A. and Sivashinsky, G. I., "Hydrodynamic Instabilities in Flame Fronts: Breathing Solutions," *Combust. Sci. Tech.*, 46, pp. 109−111 (1986).
25. Thual, O., Frisch, U. and Henon, M., "Application of Pole Decomposition to an Equation Governing the Dynamics of Wrinkled Flame Fronts," *J. Physique,* 46, pp. 1485−1494 (1985).
26. Joulin, G., "Nonlinear Hydrodynamic Instability of Expanding Flames: Intrinsic Dynamics," *Phys. Rev. E,* 50, pp. 2030−2047 (1994).
27. Mueller, C. J., Driscoll, J. F., Reuss, D. L., Drake, M. C. and Rosalik, M. E., "Vorticity Generation and Attenuation as Vortices Convert Through a Premixed Flame," *Combust. Flame*, 112, pp. 342−358 (1998).

(Manuscript received July 4, 2007,
accepted for publication November 13, 2007.)